RESEARCH ARTICLE

Association of Glymphatic Function With Clinical Characteristics in Patients With Clinical and Asymptomatic Creutzfeldt-Jakob Disease

Zhongyun Chen, MD, PhD, Deming Jiang, MD, PhD, Yu Kong, MD, PhD, Jing Zhang, MD, PhD, Chu Min, MD, PhD, Sheng Bi, MM, Shaozhen Yan, PhD, Hong Ye, MD, PhD, Junjie Li, MD, PhD, Lin Wang, MD, PhD, Jie Lu, MD, PhD,* and Liyong Wu, MD, PhD*

Neurology® 2025;104:e210055. doi:10.1212/WNL.0000000000210055

Correspondence
Dr. Wu
wmywly@hotmail.com
or Dr. Lu
imaginglu@hotmail.com

Abstract

Background and Objectives

Abnormal glymphatic system–related proteins have been identified in a small-scale pathologic study of patients with Creutzfeldt-Jakob disease (CJD). However, it remains unclear whether glymphatic dysfunction occurs in vivo in patients with CJD and whether this decline begins during the preclinical stage. This study aimed to investigate the relationship between glymphatic dysfunction and clinical characteristics in patients with CJD, as well as potential glymphatic impairment in preclinical CJD.

Methods

This prospective cohort study recruited patients with CJD and healthy controls (HCs) from the Department of Neurology at Xuanwu Hospital, Capital Medical University, Beijing, China, from 2018 to 2022. In addition, a family with preclinical genetic CJD carrying the G114V pathogenic variant was followed over 6 years with 3 evaluations. All participants underwent diffusion tensor imaging along the perivascular space (DTI-ALPS) to measure glymphatic function in vivo and ^{18}F-fludeoxyglucose-PET to identify CJD-related metabolic patterns. Associations between the DTI-ALPS index and Medical Research Council Prion Disease Rating Scale (MRC-PDRS) score were evaluated using multiple linear regression.

Results

We enrolled 35 patients with CJD (mean age 59.6 ± 10.7 years, 40% female, with the time from onset to glymphatic dysfunction assessment averaging 39% of the total disease course), 28 age-matched and sex-matched HCs, and a family with preclinical genetic CJD consisting of 7 carriers and 7 noncarriers. Patients with CJD exhibited lower DTI-ALPS values compared with HCs ($p < 0.001$). Partial correlation analyses revealed significant correlations between the DTI-ALPS index and MRC-PDRS score ($r = 0.346$, $p = 0.049$) and disease progression ($r = -0.468$, $p = 0.006$), but not with disease duration or cognitive severity after adjusting for age and sex. Multivariate linear analysis demonstrated that poorer MRC-PDRS scores ($\beta = 0.702$, $p = 0.014$) were associated with a lower DTI-ALPS index. The DTI-ALPS index of asymptomatic G114V carriers showed no significant difference compared with noncarriers. However, a preclinical CJD case exhibited an 8.2% decrease in the DTI-ALPS index 3.3 years before onset. No significant correlation was found between regional metabolic standardized uptake value ratios and DTI-ALPS index.

Discussion

Our study indicates that glymphatic dysfunction is associated with CJD severity and disease progression. Glymphatic dysfunction may occur in the preclinical stage, but these findings should be interpreted with caution because they are based on individual findings.

RELATED ARTICLE

Editorial
Diffusion Tensor Image Analysis of Glymphatic Dysfunction in Creutzfeldt-Jakob Disease
Page e210148

*These authors contributed equally to this work as co-corresponding authors.

From the Department of Neurology (Z.C., D.J., Y.K., J.Z., C.M., H.Y., J. Li, L. Wang, L. Wu), and Department of Radiology and Nuclear Medicine (S.B., S.Y., J. Lu), Xuanwu Hospital, Capital Medical University, Beijing, China.

Go to Neurology.org/N for full disclosures. Funding information and disclosures deemed relevant by the authors, if any, are provided at the end of the article.

Glossary

AQP4 = aquaporin-4; **CJD** = Creutzfeldt-Jakob disease; **CJDRP** = CJD-related pattern; **DTI-ALPS** = diffusion tensor imaging along the perivascular space; **DWI** = diffusion-weighted imaging; **FA** = fractional anisotropy; **FDG** = fludeoxyglucose; **FOV** = field of view; **gCJD** = genetic CJD; **HC** = healthy control; **ISF** = interstitial fluid; **JHU** = Johns Hopkins University; **MMSE** = Mini-Mental State Examination; **MNI** = Montreal Neurological Institute; **MoCA** = Montreal Cognitive Assessment; **MRC-PDRS** = Medical Research Council Prion Disease Rating Scale; **NC** = normal control; **PrP^{Sc}** = scrapie prion protein; **ROI** = region of interest; **RT-QuIC** = real-time quaking-induced conversion; **sCJD** = sporadic CJD; **SUVR** = standardized uptake value ratio; **TE** = echo time; **TR** = repetition time.

Introduction

Creutzfeldt-Jakob disease (CJD), the most common prion disease in humans, is a rare and fatal neurodegenerative condition characterized by the accumulation of scrapie prion protein (PrP^{Sc}) in the brain, resulting in nerve cell damage and the development of pathology and clinical symptoms.[1] The clearance of PrP^{Sc} is crucial for slowing down or preventing the neurodegenerative processes and disease-related clinical disabilities in patients with CJD.

The recently discovered "waste clearance" system in the brain, known as the glymphatic system, plays a pivotal role in removing endogenous and exogenous metabolites and maintaining homeostasis.[2-4] CSF enters the brain parenchyma through the perivascular space surrounding arteries; undergoes rapid exchange with interstitial fluid facilitated by aquaporin-4 (AQP4) in astrocytes; and eventually drains into the venous perivascular space, meninges, and cervical lymphatics.[2] Studies on $AQP4^{-/-}$ mice have shown that the absence of perivascular AQP4 impairs glymphatic transport and clearance capacity.[5,6] Recent findings have indicated a significant upregulation of AQP4 expression in the brains of individuals with various prion diseases.[7-9] In addition, a previous small-scale (n = 3) pathologic study identified abnormal expression of glymphatic system–related proteins in patients with sporadic CJD (sCJD).[10] However, it remains unclear whether glymphatic dysfunction occurs in vivo in patients with CJD and whether this decline begins during the preclinical stage.

Diffusion tensor imaging along the perivascular space (DTI-ALPS) has emerged as a noninvasive method for estimating human glymphatic activity. DTI-ALPS assesses the movement of water molecules in different directions along the perivascular space by measuring diffusivity, a critical process within the glymphatic pathway.[11] Moreover, the DTI-ALPS index has been linked to glymphatic clearance as evidenced by glymphatic MRI after intrathecal gadolinium administration.[12] Consequently, DTI-ALPS has become a valuable tool for evaluating glymphatic function, with its clinical validity demonstrated in various neurologic disorders such as Alzheimer disease,[13] Parkinson disease,[14] and frontotemporal dementia.[15]

In this prospective study, we aimed to investigate glymphatic function in CJD using the DTI-ALPS index. Our objectives included examining glymphatic dysfunction in patients with CJD and its correlation with clinical disabilities, investigating potential glymphatic impairment in a family with preclinical genetic CJD (gCJD) carrying the G114V pathogenic variant, and exploring the relationship between glymphatic system damage and metabolic-related regions in CJD. By addressing these objectives, we aim to provide insights into the pathophysiology of CJD and its potential implications for therapeutic interventions.

Methods

The study was monitored and approved by the institutional review boards of Xuanwu Hospital, Capital Medical University. Written informed consent was obtained from all living participants or their legal guardians. All investigations were conducted according to the principles of the Declaration of Helsinki.

Participants

Patients with CJD were prospectively recruited from the Department of Neurology at Xuanwu Hospital, Capital Medical University, between July 2018 and December 2022. The diagnosis of sCJD followed the established diagnostic criteria.[16] Genetic prion diseases were identified by the presence of definite *PRNP* pathogenic variants. Patients were regularly followed up every 3 months until death, either in the clinic or by telephone, to ensure a precise diagnosis and monitor changes in their condition. The exclusion criteria for patients with CJD were as follows: (1) refusal to participate; (2) inability to complete an MRI scan; (3) diagnosis of potential Hashimoto encephalopathy, viral or autoimmune encephalitis, paraneoplastic syndromes, and others; and (4) patients who clinically improved, received a clear diagnosis of another disease during the follow-up period, or were lost to follow-up. Finally, 35 patients with CJD were included in this study. Among them, 25 were diagnosed with probable sCJD and 10 were diagnosed with gCJD, with 6 cases of E200K, 2 cases of T188K, 1 case of 7-OPRI, and 1 case of V180I. 7 carriers of the asymptomatic prion protein gene (*PRNP*) G114V pathogenic variant and 7 noncarriers from the same family with gCJD were included in the study. The clinical manifestations and genetic analysis of

this family have been previously reported.[17,18] In addition, 28 healthy controls (HCs) were age-matched and sex-matched to the cases and recruited from adjacent communities. These controls had no neurologic concerns and performed within the normal range on neuropsychological tests (Mini-Mental State Examination [MMSE] score: ≥24).

Clinical Screening

All patients underwent a comprehensive clinical assessment, including cognitive evaluations such as the MMSE and the Montreal Cognitive Assessment (MoCA). Disease severity was determined using the Medical Research Council Prion Disease Rating Scale (MRC-PDRS), a composite scale ranging from 0 (indicating a comatose state) to 20 (representing independence in activities of daily living).[19] Disease duration was defined as the time from onset of symptoms to death. The degree of disease progression was defined as the interval between onset and DTI examination divided by the disease duration. To quantify the extent of high diffusion-weighted imaging (DWI) signal, each brain region exhibiting high DWI signal was assigned 1 point: frontal lobe, temporal lobe, parietal lobe, occipital lobe, caudate nucleus, putamen, and thalamus. If these regions appeared bilaterally, 2 points were assigned.[20] In addition, evaluations included EEG, CSF analysis (including 14-3-3 protein concentration), real-time quaking-induced conversion (RT-QuIC), and *PRNP* variation analysis. For G114V pathogenic variant carriers and noncarriers in the same family, a 4-year longitudinal follow-up was conducted, during which they underwent neuropsychological examinations and fludeoxyglucose (FDG)-PET scans every 2 years.

MRI Protocols

All participants underwent a comprehensive brain imaging session using a hybrid 3.0T time-of-flight PET/MRI scanner (SIGNA PET/MR; GE Healthcare, Milwaukee, WI). Each participant fasted for at least 6 hours to ensure that serum glucose levels were less than 9 mmol/L, followed by intravenous injection of 3.7 MBq/kg of ^{18}F-FDG. Participants were instructed to wait for at least 30 minutes before FDG administration and during the brain uptake phase. PET and MRI data were acquired simultaneously with the aid of a vendor-supplied 19-channel head and neck union coil. The MRI protocol included the following sequences: A 3-dimensional T1-weighted sagittal scan was conducted with the following parameters: repetition time (TR) = 6.9 milliseconds, echo time (TE) = 2.98 milliseconds, flip angle = 12°, inversion time = 450 milliseconds, matrix size = 256 × 256, field of view (FOV) = 256 × 256 mm^2, slice thickness = 1 mm, 192 sagittal slices with no gap, and voxel size = 1 × 1 × 1 mm^3. A DTI scan was performed using a spin-echo echo-planar imaging sequence with 5 b-values of 0 s/mm^2 and 30 b-values of 1,000 s/mm^2 along noncollinear directions. The parameters were as follows: TR = 16,500 milliseconds, TE = 74.6 milliseconds, matrix size = 112 × 112, FOV = 256 × 256 mm^2, slice thickness = 2 mm, 70 axial slices with no slice gap, and number of excitations = 1. A static ^{18}F-FDG PET scan was conducted with a matrix size of 192 × 192, FOV of 350 × 350 mm^2, and pixel size of 1.82 × 1.82 × 2.78 mm^3. Corrections for random coincidences, dead time, scatter, and photon attenuation were applied to the PET data. Foam pads were placed inside the head coil during the MRI scanning session to minimize potential head motion.

Quantification of Cortical Thickness and Cortical Volume

We used the T1-FreeSurfer pipeline of Clinica 0.7.1 to extract whole-brain cortical thickness and cortical volume. This process involves segmenting subcortical structures, extracting cortical surfaces, estimating cortical thickness, and spatially normalizing onto the FreeSurfer surface template (FsAverage).

Quantification of DTI-ALPS Index

The DTI-ALPS index was calculated following a previous study.[21] In brief, the preprocessing of DWI was conducted in the Clinica (version: 0.7.1) platform based on the DWI-preprocessing-using-T1 pipeline and DWI-DTI pipeline.[22] Subsequently, each participant's fractional anisotropy (FA) map was aligned to the FA map of the Johns Hopkins University (JHU) atlas template using the ANTs SyN algorithm as a reference to obtain the estimated nonlinear deformation that then was applied to other diffusion metric maps. Based on JHU atlas labeling, regions of interest (ROIs) with a thickness of 3 mm were extracted bilaterally within the projection (anterior, superior, and posterior corona radiata) and association fibers (superior longitudinal fasciculus) at the level of the lateral ventricle (Montreal Neurological Institute [MNI] coordinates z = 26). The DTI-ALPS index was then calculated as the average of both sides (eFigure 1). The DTI-ALPS index was computed by taking the ratio of the mean diffusivity values across voxels in the projection and association ROIs on the Dxx map (Dxxproj, Dxxassoc) and the mean diffusivity values across voxels in the projection ROI on the Dyy map (Dyyproj) and the association ROI on the Dzz map (Dzzassoc), as follows[11]:

$$\text{DTI-ALPS} = \frac{\text{mean}(\text{Dxxproj}, \text{Dxxassoc})}{\text{mean}(\text{Dyyproj}, \text{Dzzassoc})} \quad (1)$$

PET Image Preprocessing

PET images were preprocessed using SPM12, implemented in MATLAB (MathWorks, Natick, MA). After spatial normalization of the structural MR images to standard MNI space using diffeomorphic anatomical registration through exponentiated lie algebra normalization, the transformation parameters determined by the T1-weighted image spatial normalization were applied to the coregistered PET images for PET spatial normalization. The images were then smoothed using an 8-mm full-width half-maximum isotropic Gaussian kernel. To identify and characterize specific spatial covariance patterns related to CJD, an automated SSM/PCA procedure[23] was used to analyze FDG-PET scans of patients and normal controls (NCs).[24] Gray matter was automatically extracted using a customized mask based on an automated anatomical labeling atlas, followed by automatic principal component analysis on a group of patients with CJD and NCs.

Table 1 Demographic and Clinical Features of Patients With CJD and HCs

Characteristic	CJD (n = 35)	HCs (n = 28)	*p* Value
Patient information			
Age at onset, y, mean ± SD	59.6 ± 10.7	60.2 ± 8.4	0.824
Sex, male, n (%)	21 (60.0)	11 (34.3)	0.102
Onset to DTI, d, median (IQR)	71.0 (50.0–278.0)	—	—
Duration, d, median (IQR)	365.0 (198.0–558.0)	—	—
Degree of disease progression, mean ± SD	0.39 ± 0.24	—	—
Clinical features at presentation, n (%)			
Cognitive	33 (94.2)	—	—
Psychiatric	14 (40.0)	—	—
Visual	11 (31.4)	—	—
Extrapyramidal	12 (34.3)	—	—
Pyramidal	19 (54.2)	—	—
Cerebellar	17 (48.6)	—	—
Myoclonus	15 (42.9)	—	—
Mutism	4 (11.4)	—	—
Scale evaluation			
MMSE score, median (IQR)	8.0 (0–16.0)	29.0 (28.0–30.0)	<0.001
MoCA score, median (IQR)	3.0 (0–6.0)	25.0 (24.0–27.0)	<0.001
MRC-PDRS score, median (IQR)	10.0 (3.0–18.0)	—	—
CSF 14-3-3 positive (n = 34), n (%)	20 (58.8)	—	—
Periodic discharges on EEG, n (%)	19 (54.2)	—	—
Hyperintensity on DWI, n (%)	34 (97.1)	—	—
Number of involved lobes	8 (5.8–9.0)	—	—
Positive RT-QuIC (n = 9), n (%)	9 (100.0)	—	—
Codon 129M/M genotype, n (%)	35 (100.0)	—	—

Abbreviations: CJD, Creutzfeldt-Jakob disease; DTI, diffusion tensor imaging; DWI, diffusion-weighted imaging; HCs, healthy controls; IQR, interquartile range; M/M, methionine homozygosity; MMSE, Mini-Mental State Examination; MoCA, Montreal Cognitive Assessment; MRC-PDRS, Medical Research Council Prion Disease Rating Scale; RT-QuIC, real-time quaking-induced conversion.

The linearly independent covariance patterns (principal components) obtained were linearly combined into a single spatial covariance CJD-related pattern (CJDRP) using the Akaike information criterion.[25,26] The expression of CJDRP (patient scores) was calculated for each patient's scan and z-transformed with respect to the identified NC group. Finally, PET scan intensity was normalized using a whole-cerebellum reference region to create standardized uptake value ratio (SUVR) images. The SUVR was then extracted from these brain regions for each patient.

Statistical Analysis

All statistical analyses were conducted using SPSS version 20.0 (IBM Corp., Armonk, NY). 2-sample *t* tests or Mann–Whitney *U* tests for continuous variables and χ^2 tests for categorical variables were used for between-group comparisons. For the DTI-ALPS index, a general linear model was used to compare the metrics between patients with CJD and HCs, with age and sex included as covariates. Partial Pearson correlation analysis was performed to assess the relationship between glymphatic measures and clinical parameters, regional SUVR values adjusted for age and sex. Univariate linear regression analysis was conducted to examine the correlation between the DTI-ALPS index of patients with CJD and clinical data. Subsequently, a multivariate linear analysis was used to explore the independent predictors of the DTI-ALPS index in patients with CJD. Variables with $p < 0.1$ in the univariate regression analysis

Figure 1 DTI-ALPS Index of Patients With CJD and HCs

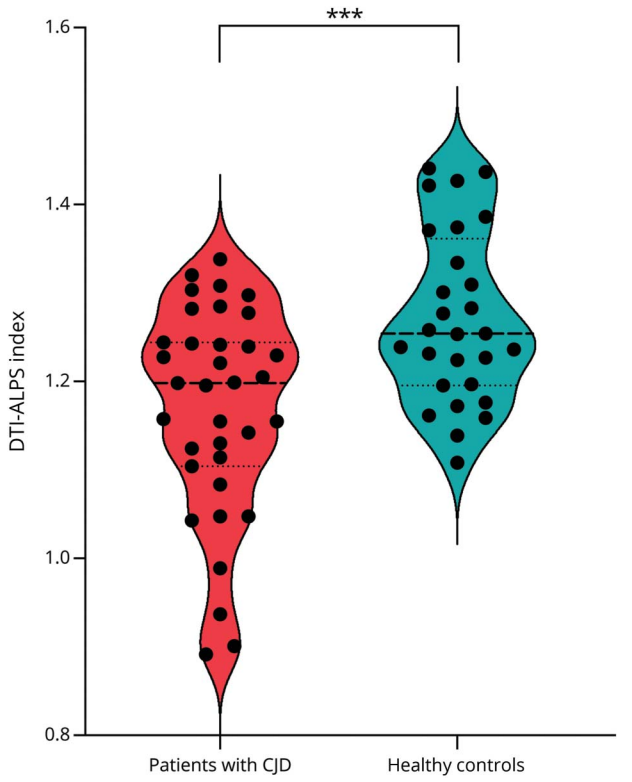

Compared with HCs, patients with CJD had a significantly lower DTI-ALPS index. CJD, Creutzfeldt-Jakob disease; DTI-ALPS, diffusion tensor imaging along the perivascular space; HC, healthy control.

were included in the multivariate regression analysis using a backward elimination approach. Within the family with the G114V pathogenic variant, participants whose DTI-ALPS index decline rate was 2 SDs greater than the mean (calculated based on the remaining participants) were considered fast decliners.[17] Statistical significance was set at $p < 0.05$.

Data Availability

Data are available on reasonable request. The data in this research can be obtained by emailing the corresponding author.

Results

Demographic and Clinical Features

Table 1 summarizes the demographic and clinical information of the patients with CJD and HCs. Among the 35 patients, there were 21 men (60%) and 14 women (40%), with a mean age of 59.6 years and a median survival time of 1.0 year. Most of the included patients with CJD were in the early or middle stages of the disease, with the time from onset to DTI examination accounting for 39% of the total course of the disease. The proportions of CSF 14-3-3 protein positivity, periodic discharges on EEG, hyperintensity on DWI, and positive CSF/skin RT-QuIC were 58.8%, 54.2%, 97.1%, and 100%, respectively. All patients were homozygous for methionine at codon 129 (129M/M). HCs were age-matched and sex-matched with the patients with CJD ($p > 0.05$). Patients with CJD had lower MMSE and MoCA scores compared with HCs ($p < 0.01$).

Comparison of Glymphatic Function Between Patients With CJD and HCs

A negative correlation was observed between age and the DTI-ALPS index ($r = -0.604$, $p < 0.001$) in CJD (eFigure 2). Men had a significantly higher DTI-ALPS index than women ($p = 0.024$; eFigure 2). Patients with CJD showed a significantly lower DTI-ALPS index compared with HCs ($p < 0.001$; Figure 1), with statistical significance persisting after adjusting for age and sex ($p < 0.001$). No differences were found in the DTI-ALPS index between patients with sCJD and gCJD (1.15 ± 0.12 vs 1.20 ± 0.11, $p = 0.268$).

Correlation Between Glymphatic Function and Clinical Parameters

In patients with CJD, the DTI-ALPS index was significantly correlated with MMSE score ($r = 0.335$, $p = 0.049$), MRC-PDRS score ($r = 0.432$, $p = 0.009$), degree of disease progression ($r = -0.372$, $p = 0.028$), and disease duration ($r = 0.339$, $p = 0.046$) (Figure 2). After adjusting for age and sex, the DTI-ALPS index was only significantly correlated with the MRC-PDRS score ($r = 0.346$, $p = 0.049$) and degree of disease progression ($r = -0.468$, $p = 0.006$). There were no correlations observed between the DTI-ALPS index and MoCA score, time from onset to DTI examination, quantification of hyperintensity on DWI, cortical thickness, and cortical volume (Figure 2).

Univariate analysis revealed that MMSE ($\beta = 0.360$, $p = 0.033$) and MRC-PDRS ($\beta = 0.510$, $p = 0.002$) scores were associated with the DTI-ALPS index while the MoCA score ($\beta = 0.301$, $p = 0.079$) tended to be associated with the DTI-ALPS index in patients with CJD. Subsequently, multivariate analysis including age, sex, MMSE score, MoCA score, and MRC-PDRS score as predictive factors showed that a poorer MRC-PDRS score ($\beta = 0.702$, $p = 0.014$) was associated with a lower DTI-ALPS index in patients with CJD.

Trajectory of Glymphatic Function Changes of Asymptomatic gCJD

Demographic data and cognitive status of carriers and noncarriers from a G114V pathogenic variant family were assessed at both baseline and follow-up visits, as summarized in eTable 1. The expected age at onset for this family was 43.9 years (calculated by the mean onset age of 9 deceased CJD family members), with 3 individuals (carriers 1, 2, and 3) nearing or exceeding this age. Among them, carrier 1 completed only 2 DTI assessments. Among all carriers, only carrier 1 exhibited a significant glymphatic function change (Figure 3), with the DTI-ALPS index decreasing by 8.2% compared with the previous assessment—exceeding 2 SDs

Figure 2 Correlations of the DTI-ALPS Index With Clinical Characteristics in CJD

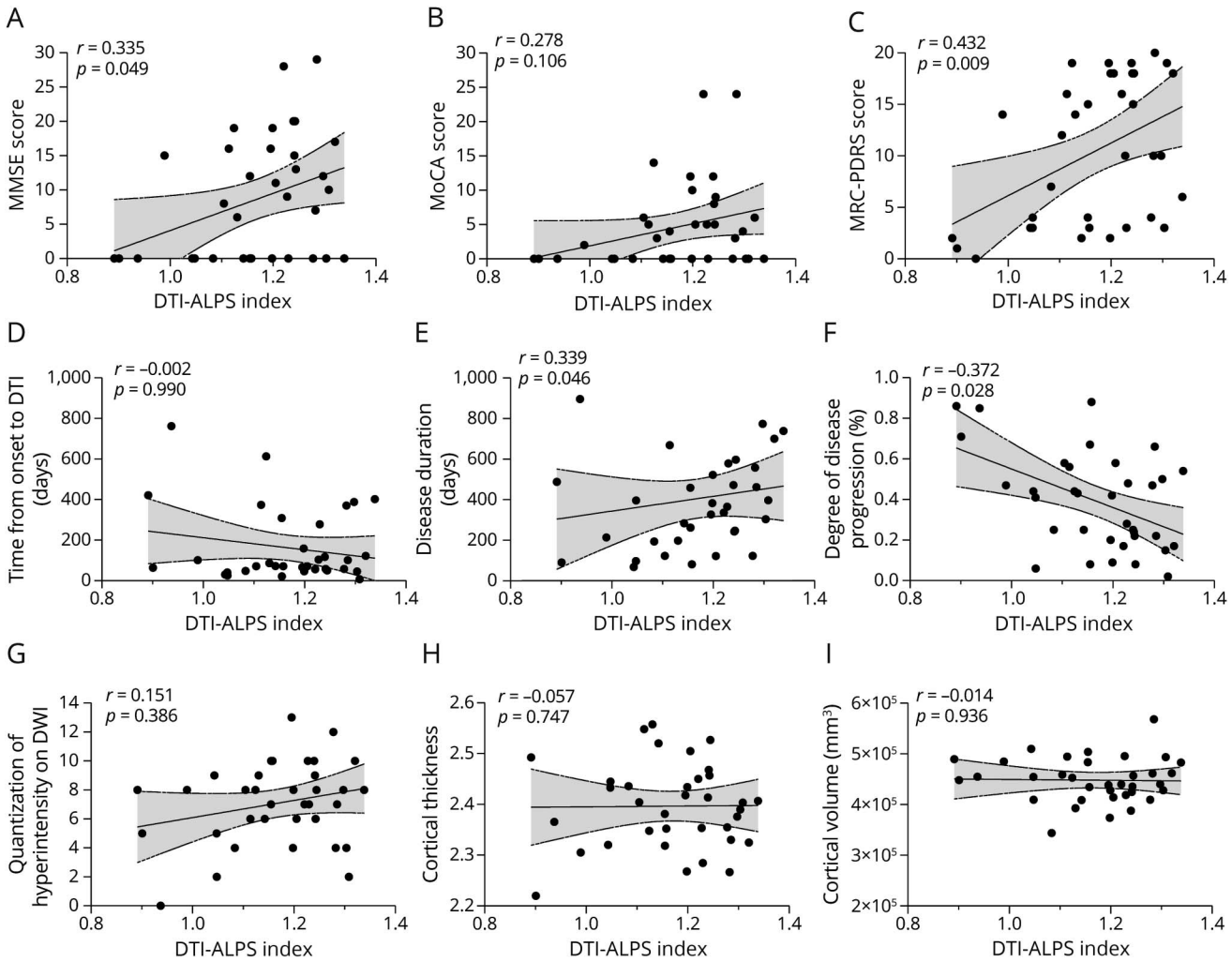

The DTI-ALPS index was significantly correlated with MMSE score (A), MRC-PDRS score (C), disease duration (E), and degree of disease progression (F). However, it was not correlated with MoCA score (B), time from onset to DTI examination (D), quantification of hyperintensity on DWI (G), cortical thickness (H), or cortical volume (I). CJD, Creutzfeldt-Jakob disease; DTI-ALPS, diffusion tensor imaging along the perivascular space; DWI, diffusion-weighted imaging; MMSE, Mini-Mental State Examination; MoCA, Montreal Cognitive Assessment; MRC-PDRS, Medical Research Council Prion Disease Rating Scale.

greater the mean calculated based on carriers 2–6—and significantly lower than that of the noncarrier's group ($p < 0.001$). This patient developed clinical symptoms in 3.3 years after the first follow-up. Although carrier 2 was identified in an earlier study with varying degrees of metabolic decline in brain regions, greater than 2 SDs above the mean compared with other carriers,[17] as of March 2024 (3 years after the second follow-up), this patient has not developed symptoms. This may suggest that rapid changes in glymphatic function could be more predictive of disease onset than PET metabolic values. However, these results should be interpreted with caution because they are based on individual findings.

Correlation Between Regional Glymphatic Function and Metabolic Pattern

Compared with the HCs, the patients with CJD exhibited decreased cortical and subcortical metabolism across a wide range of regions, particularly in the precuneus, angular gyrus, posterior cingulate gyrus, middle frontal gyrus, striatum, and thalamus (Figure 4A). These findings are consistent with those of previous studies. The expression pattern of this metabolic alteration significantly distinguished patients with CJD from HCs ($p < 0.001$, Figure 4B). However, no significant correlation was found between CJDRP expression value and regional metabolic SUVRs and the DTI-ALPS index in our data set (Figure 4C).

Discussion

In this study, we used the DTI-ALPS index to demonstrate in vivo glymphatic dysfunction in patients with clinical and asymptomatic CJD. We identified a correlation between glymphatic dysfunction and disease severity, as well as the stage of disease progression, in patients with symptomatic

Figure 3 Trajectory of Glymphatic Function Changes in G114V Pathogenic Variant Carriers and Noncarriers From the Same Family

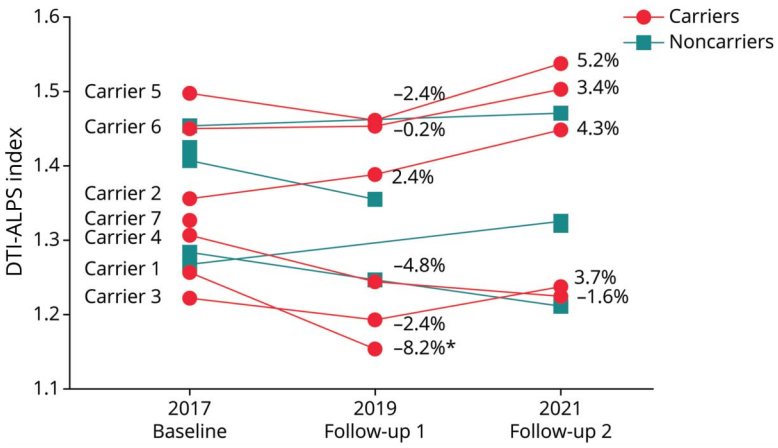

Although there were varying degrees of fluctuations in glymphatic function over the 3 assessments for both groups, there was no significant overall difference in the DTI-ALPS index between the 2 groups. In the figure, we listed the percentage change rate of DTI-ALPS index in asymptomatic *PRNP* carriers between the 2 adjacent assessments. Carrier 1 underwent only 2 DTI assessments, and the significant decline (*) in the DTI-ALPS index was observed at the second assessment. DTI-ALPS, diffusion tensor imaging along the perivascular space.

CJD. Furthermore, our results suggest that glymphatic dysfunction may precede the onset of symptoms in a carrier of an asymptomatic *PRNP* pathogenic variant. These findings underscore the potential association between glymphatic dysfunction and CJD pathology.

The glymphatic system clears waste from the interstitial fluid (ISF) of the brain through exchange with CSF, a process in which AQP4 plays a key role, and is crucial for maintaining brain homeostasis. Changes in AQP4 expression are associated with aging or pathology and are linked to a decline in this system's function in both animal models and patient brains.[27,28] In disease states, AQP4 expression in the brain increases, but glymphatic clearance is compromised, often due to the loss of polarity of AQP4 endfeet.[29] Abnormal AQP4 polarity distribution in AD animal models and patients aggregates around Aβ deposition sites, potentially slowing fluid flow and accelerating disease progression.[30,31] Similar observations were made in patients with CJD, with AQP4 aggregation found within or around prion plaques.[8] Studies have indicated that overexpression and mislocalization of AQP4 in prion-infected mice and sCJD can be detected, with activation of the glymphatic system increasing the PrP^{Sc} clearance rate, thereby delaying disease onset. These findings suggest that not only early detection of glymphatic dysfunction aids in early diagnosis but also improving glymphatic function may serve as a therapeutic target to slow the neurodegenerative process in patients with CJD.

Similar to other neurodegenerative diseases, patients with CJD may experience a prolonged prodromal phase, suggesting a multi-step process for disease onset.[32] Our findings demonstrate a significant decrease in the DTI-ALPS index several years before symptom onset in a preclinical CJD case. This observation is in line with studies in animal models of prion diseases, suggesting the presence of glymphatic dysfunction during the preclinical stage.[10] Previous research has indicated that astrocytes respond to prion infection before neurons and even microglia.[33] Elevated levels of glial fibrillary acidic protein, an astrocyte marker, have been detected several years before the clinical onset of inherited prion diseases.[32] Astrocytes play a crucial role in the periarterial CSF in-flow and perivenous ISF out-flow pathways of the glymphatic system.[2] In a mouse model of prion disease, a significant reduction in the localization of AQP4 in astrocytic endfeet was observed during the presymptomatic phase, indicating early loss of astrocyte polarity in the disease process.[9] Therefore, these studies support the notion that glymphatic dysfunction may manifest before disease onset in patients with CJD. A recent study on AD found that glymphatic dysfunction might precede amyloid pathology, indirectly supporting our conclusion.[13]

We assessed the correlation between glymphatic function and clinical characteristics of CJD and found that the DTI-ALPS index is correlated with MRC-PDRS scores and disease progression, but not with cognitive impairment or survival time. The lack of correlation with cognitive impairment could be due to the fact that approximately a third of the MRC-PDRS score maps to cognitive functioning, and with 42.9% of patients having a cognitive assessment score of 0, the sample may not accurately reflect this relationship. The lack of correlation with survival time may be due to several factors: MRC-PDRS scores and survival time are only moderately correlated ($r = 0.432$) in our study, and survival time can be influenced by pathologic subtypes and intensive life-sustaining treatments. For example, the clinically diagnosed MM2 subtype sCJD, which might exceed one-fourth of cases in our center, typically progresses more slowly with longer disease duration,[34] and patients receiving intensive life-sustaining treatments also have longer survival time.[35] In addition, the relatively small sample size in this study might lead to statistical results being affected by individual outliers.

Figure 4 CJDRP and Its Spatial Correlation With Glymphatic Function

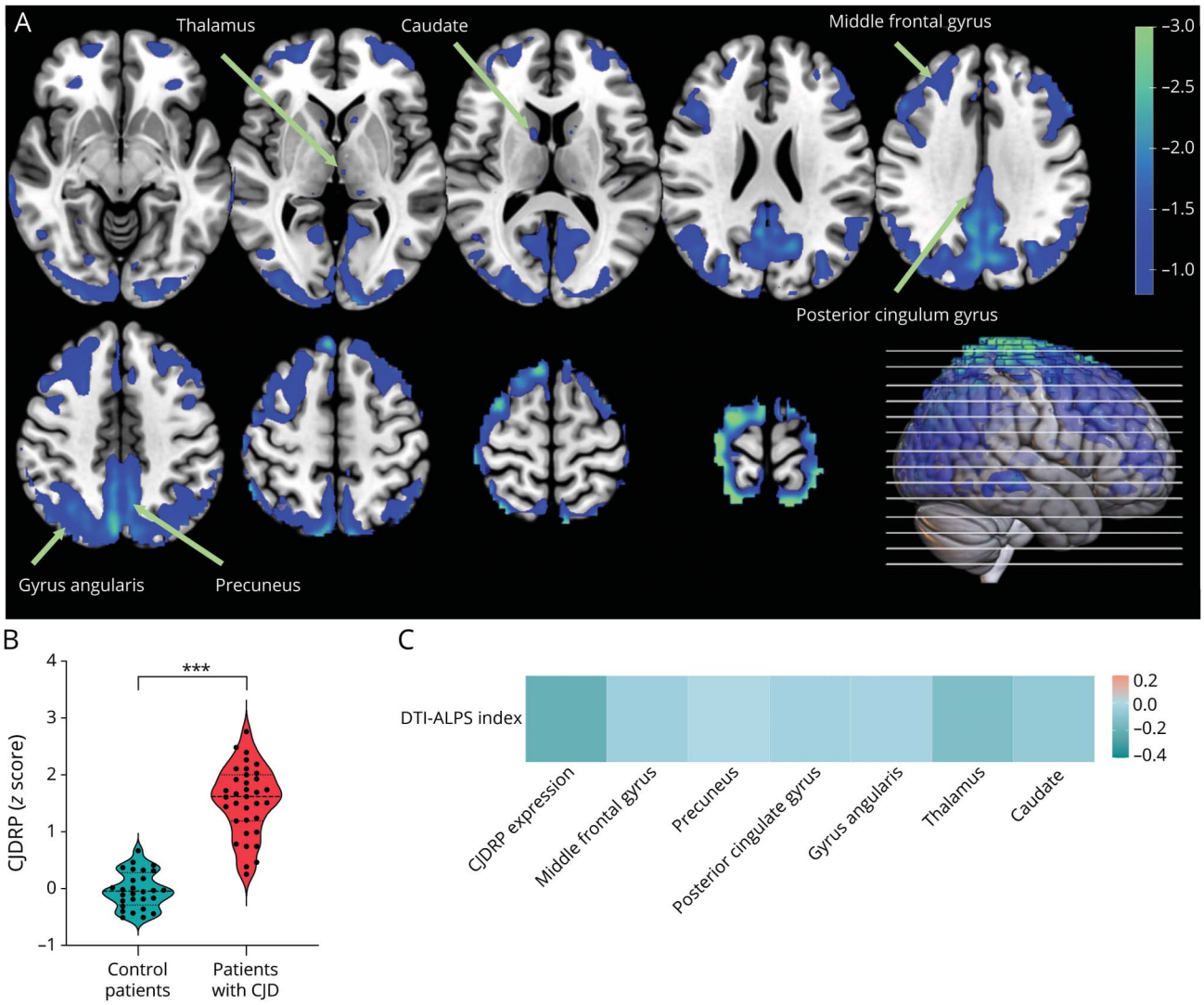

(A) The CJDRP was identified from ^{18}F-FDG PET data of 35 patients with CJD and 28 age-matched and sex-matched healthy controls using spatial covariance analysis (SSM/PCA). Voxel weights on metabolic network regions were determined based on bootstrap estimation. Metabolic reductions were observed bilaterally in the precuneus, angular gyrus, posterior cingulate gyrus, middle frontal gyrus, striatum, and thalamus. (B) Individual expression of CJDRP significantly ($p < 0.001$, the Student t test between groups) distinguished patients with CJD from healthy controls. (C) Heatmap shows no correlation between DTI-ALPS and the expression of CJDRP, and the regional SUVR values of 6 ROIs in patients with CJD. CJD, Creutzfeldt-Jakob disease; CJDRP, CJD-related pattern; DTI-ALPS, diffusion tensor imaging along the perivascular space; FDG, fludeoxyglucose; ROI, region of interest; SUVR, standardized uptake value ratio.

Our study also explored the relationship between glymphatic function and regional metabolism in CJD. Regrettably, we found no correlation between the DTI-ALPS index and CJDRP expression or regional metabolism. While our findings suggest that glymphatic dysfunction may not be significantly associated with PrP^{Sc} deposition, given the assumption that the metabolic decline observed on FDG-PET is related to the neuropathology of prion diseases,[36,37] it is worth noting that there are studies indicating that FDG-PET may not accurately reflect the pathologic changes in prion diseases.[38] In addition, the DTI-ALPS index mainly represents the interstitial fluid efflux function along the perivenous space in the white matter. Glymphatic dysfunction in the cortex may differ from that in the white matter because most patients with CJD in this study had diffusion restriction gray matter lesions. FDG-PET represents neuronal activities in the cerebral cortex. Furthermore, our previous research indicated that regional rather than global glymphatic dysfunction in patients with FTD may correlate with regional protein deposition and spread.[15] Considering the significant reduction in metabolism in the parieto-occipital lobe of patients with CJD, future studies should expand the sample size and focus on regional glymphatic dysfunction.

Despite these significant findings, our study had limitations. The relatively small sample size and the lack of pathologic confirmation of sCJD, a challenge in China, are

notable limitations. However, approximately one-third of patients with sCJD underwent RT-QuIC testing, all yielding positive results. In addition, all patients were followed up until death and met clinically probable sCJD diagnostic criteria at death, enhancing the validity of our results. Our study was conducted at a single center, suggesting the need for further population-based or multicenter studies to validate our findings. Furthermore, we did not assess the relationship between sleep disturbances and glymphatic dysfunction, which has been associated with other neurodegenerative diseases.[39,40] Although sleep disturbances are a major clinical feature of E200K, we did not find differences in the DTI-ALPS index between this type of gCJD and other types of CJD in the limited data available. Future studies should consider evaluating sleep disturbances in the context of glymphatic dysfunction in CJD. Although our study suggests preclinical glymphatic dysfunction in CJD, this observation is based on a single case and continued follow-up is necessary. Finally, the DTI-ALPS index is primarily limited to white matter regions, making it difficult to fully capture the overall function of the glymphatic system, and is susceptible to confounding factors such as patient movement and blood flow changes. Although it shows associations with certain neurologic diseases, its validity and accuracy as a marker of glymphatic function remain questionable.[41] Further studies combining other noninvasive choroid plexus volume and blood oxygen level–dependent (BOLD)-CSF coupling indices, or using dynamic contrast-enhanced (DCE) MRI[42] or T1 mapping MRI techniques,[43] could provide deeper insights into CJD lymphatic function.

In conclusion, our study suggests that glymphatic dysfunction may be associated with the progression of CJD and could occur in the preclinical stage. These insights into glymphatic dysfunction in patients with CJD highlight its potential correlation with disease pathology. Further research in this area could lead to the development of new therapeutic strategies for CJD.

Study Funding

This work was supported by grants from National Natural Science Foundation of China (82271464, 81971011), Capital's Funds for Health Improvement and Research (2024-2-2018), and Beijing Postdoctoral Research Foundation (2022-ZZ-016).

Disclosure

The authors report no relevant disclosures. Go to Neurology.org/N for full disclosures.

Publication History

Received by *Neurology* June 4, 2024. Accepted in final form September 10, 2024. Submitted and externally peer reviewed. The handling editor was Associate Editor Linda Hershey, MD, PhD, FAAN.

Appendix Authors

Name	Location	Contribution
Zhongyun Chen, MD, PhD	Department of Neurology, Xuanwu Hospital, Capital Medical University, Beijing, China	Drafting/revision of the manuscript for content, including medical writing for content; major role in the acquisition of data; study concept or design; analysis or interpretation of data
Deming Jiang, MD, PhD	Department of Neurology, Xuanwu Hospital, Capital Medical University, Beijing, China	Drafting/revision of the manuscript for content, including medical writing for content; study concept or design; analysis or interpretation of data
Yu Kong, MD, PhD	Department of Neurology, Xuanwu Hospital, Capital Medical University, Beijing, China	Drafting/revision of the manuscript for content, including medical writing for content; major role in the acquisition of data
Jing Zhang, MD, PhD	Department of Neurology, Xuanwu Hospital, Capital Medical University, Beijing, China	Drafting/revision of the manuscript for content, including medical writing for content; major role in the acquisition of data
Chu Min, MD, PhD	Department of Neurology, Xuanwu Hospital, Capital Medical University, Beijing, China	Drafting/revision of the manuscript for content, including medical writing for content; major role in the acquisition of data
Sheng Bi, MM	Department of Radiology and Nuclear Medicine, Xuanwu Hospital, Capital Medical University, Beijing, China	Drafting/revision of the manuscript for content, including medical writing for content; major role in the acquisition of data
Shaozhen Yan, PhD	Department of Radiology and Nuclear Medicine, Xuanwu Hospital, Capital Medical University, Beijing, China	Drafting/revision of the manuscript for content, including medical writing for content; major role in the acquisition of data
Hong Ye, MD, PhD	Department of Neurology, Xuanwu Hospital, Capital Medical University, Beijing, China	Drafting/revision of the manuscript for content, including medical writing for content; major role in the acquisition of data
Junjie Li, MD, PhD	Department of Neurology, Xuanwu Hospital, Capital Medical University, Beijing, China	Drafting/revision of the manuscript for content, including medical writing for content; major role in the acquisition of data
Lin Wang, MD, PhD	Department of Neurology, Xuanwu Hospital, Capital Medical University, Beijing, China	Drafting/revision of the manuscript for content, including medical writing for content; major role in the acquisition of data
Jie Lu, MD, PhD	Department of Radiology and Nuclear Medicine, Xuanwu Hospital, Capital Medical University, Beijing, China	Drafting/revision of the manuscript for content, including medical writing for content; major role in the acquisition of data
Liyong Wu, MD, PhD	Department of Neurology, Xuanwu Hospital, Capital Medical University, Beijing, China	Drafting/revision of the manuscript for content, including medical writing for content; major role in the acquisition of data

References

1. Zerr I, Ladogana A, Mead S, Hermann P, Forloni G, Appleby BS. Creutzfeldt-Jakob disease and other prion diseases. *Nat Rev Dis Primers*. 2024;10(1):14. doi:10.1038/s41572-024-00497-y
2. Rasmussen MK, Mestre H, Nedergaard M. Fluid transport in the brain. *Physiol Rev*. 2022;102(2):1025-1151. doi:10.1152/physrev.00031.2020
3. Carlstrom LP, Eltanahy A, Perry A, et al. A clinical primer for the glymphatic system. *Brain*. 2022;145(3):843-857. doi:10.1093/brain/awab428
4. Xiong Y, Yu Q, Zhi H, et al. Advances in the study of the glymphatic system and aging. *CNS Neurosci Ther*. 2024;30(6):e14803. doi:10.1111/cns.14803
5. Bojarskaite L, Nafari S, Ravnanger AK, et al. Role of aquaporin-4 polarization in extracellular solute clearance. *Fluids Barriers CNS*. 2024;21(1):28. doi:10.1186/s12987-024-00527-7
6. Gomolka RS, Hablitz LM, Mestre H, et al. Loss of aquaporin-4 results in glymphatic system dysfunction via brain-wide interstitial fluid stagnation. *Elife*. 2023;12:e82232. doi:10.7554/eLife.82232
7. Costa C, Tortosa R, Rodríguez A, et al. Aquaporin 1 and aquaporin 4 overexpression in bovine spongiform encephalopathy in a transgenic murine model and in cattle field cases. *Brain Res*. 2007;1175:96-106. doi:10.1016/j.brainres.2007.06.088
8. Sadashima S, Honda H, Suzuki SO, et al. Accumulation of astrocytic aquaporin 4 and aquaporin 1 in prion protein plaques. *J Neuropathol Exp Neurol*. 2020;79:419-429. doi:10.1093/jnen/nlaa010
9. Kushwaha R, Li Y, Makarava N, et al. Reactive astrocytes associated with prion disease impair the blood brain barrier. *Neurobiol Dis*. 2023;185:106264. doi:10.1016/j.nbd.2023.106264
10. Kim YC, Won SY, Jeong BH. Altered expression of glymphatic system-related proteins in prion diseases: implications for the role of the glymphatic system in prion diseases. *Cell Mol Immunol*. 2021;18(9):2281-2283. doi:10.1038/s41423-021-00747-z
11. Taoka T, Masutani Y, Kawai H, et al. Evaluation of glymphatic system activity with the diffusion MR technique: diffusion tensor image analysis along the perivascular space (DTI-ALPS) in Alzheimer's disease cases. *Jpn J Radiol*. 2017;35(4):172-178. doi:10.1007/s11604-017-0617-z
12. Zhang W, Zhou Y, Wang J, et al. Glymphatic clearance function in patients with cerebral small vessel disease. *Neuroimage*. 2021;238:118257. doi:10.1016/j.neuroimage.2021.118257
13. Huang SY, Zhang YR, Guo Y, et al. Glymphatic system dysfunction predicts amyloid deposition, neurodegeneration, and clinical progression in Alzheimer's disease. *Alzheimers Dement*. 2024;20(5):3251-3269. doi:10.1002/alz.13789
14. Shen T, Yue Y, Ba F, et al. Diffusion along perivascular spaces as marker for impairment of glymphatic system in Parkinson's disease. *NPJ Parkinsons Dis*. 2022;8(1):174. doi:10.1038/s41531-022-00437-1
15. Jiang D, Liu L, Kong Y, et al. Regional glymphatic abnormality in behavioral variant frontotemporal dementia. *Ann Neurol*. 2023;94(3):442-456. doi:10.1002/ana.26710
16. CDC's Diagnostic Criteria for Creutzfeldt-Jakob Disease (CJD). 2018. Accessed October 22, 2024. cdc.gov/creutzfeldt-jakob/hcp/clinical-overview/diagnosis.html
17. Chu M, Chen Z, Nie B, et al. A longitudinal (18)F-FDG PET/MRI study in asymptomatic stage of genetic Creutzfeldt-Jakob disease linked to G114V mutation. *J Neurol*. 2022;269(11):6094-6103. doi:10.1007/s00415-022-11288-4
18. Lu H, Jing D, Chen Y, et al. Metabolic changes detected by 18F-FDG PET in the preclinical stage of familial Creutzfeldt-Jakob disease. *J Alzheimers Dis*. 2020;77(4):1513-1521. doi:10.3233/JAD-200576
19. Thompson AG, Lowe J, Fox Z, et al. The Medical Research Council prion disease rating scale: a new outcome measure for prion disease therapeutic trials developed and validated using systematic observational studies. *Brain*. 2013;136(4):1116-1127. doi:10.1093/brain/awt048
20. Park HY, Suh CH, Shim WH, et al. Prognostic value of diffusion-weighted imaging in patients with newly diagnosed sporadic Creutzfeldt-Jakob disease. *Eur Radiol*. 2022;32(3):1941-1950. doi:10.1007/s00330-021-08363-1
21. Taoka T, Ito R, Nakamichi R, et al. Reproducibility of diffusion tensor image analysis along the perivascular space (DTI-ALPS) for evaluating interstitial fluid diffusivity and glymphatic function: CHanges in Alps index on Multiple conditiON acquIsition eXperiment (CHAMONIX) study. *Jpn J Radiol*. 2022;40(2):147-158. doi:10.1007/s11604-021-01187-5
22. Routier A, Burgos N, Díaz M, et al. Clinica: an open-source software platform for reproducible clinical neuroscience studies. *Front Neuroinform*. 2021;15:689675. doi:10.3389/fninf.2021.689675
23. Center for Neurosciences at The Feinstein Institutes for Medical Research. Accessed October 22, 2024. feinsteinneuroscience.org.
24. Spetsieris PG, Ma Y, Dhawan V, Eidelberg D. Differential diagnosis of parkinsonian syndromes using PCA-based functional imaging features. *Neuroimage*. 2009;45(4):1241-1252. doi:10.1016/j.neuroimage.2008.12.063
25. Tomše P, Jensterle L, Grmek M, et al. Abnormal metabolic brain network associated with Parkinson's disease: replication on a new European sample. *Neuroradiology*. 2017;59(5):507-515. doi:10.1007/s00234-017-1821-3
26. Rus T, Mlakar J, Ležaić L, et al. Sporadic Creutzfeldt-Jakob disease is associated with reorganization of metabolic connectivity in a pathological brain network. *Eur J Neurol*. 2023;30(4):1035-1047. doi:10.1111/ene.15669
27. Venkat P, Chopp M, Zacharek A, et al. White matter damage and glymphatic dysfunction in a model of vascular dementia in rats with no prior vascular pathologies. *Neurobiol Aging*. 2017;50:96-106. doi:10.1016/j.neurobiolaging.2016.11.002
28. Kress BT, Iliff JJ, Xia M, et al. Impairment of paravascular clearance pathways in the aging brain. *Ann Neurol*. 2014;76(6):845-861. doi:10.1002/ana.24271
29. Zeppenfeld DM, Simon M, Haswell JD, et al. Association of perivascular localization of aquaporin-4 with cognition and Alzheimer disease in aging brains. *JAMA Neurol*. 2017;74(1):91-99. doi:10.1001/jamaneurol.2016.4370
30. Yang J, Lunde LK, Nuntagij P, et al. Loss of astrocyte polarization in the tg-ArcSwe mouse model of Alzheimer's disease. *J Alzheimers Dis*. 2011;27(4):711-722. doi:10.3233/jad-2011-110725
31. Peng W, Achariyar TM, Li B, et al. Suppression of glymphatic fluid transport in a mouse model of Alzheimer's disease. *Neurobiol Dis*. 2016;93:215-225. doi:10.1016/j.nbd.2016.05.015
32. Mok TH, Nihat A, Majbour N, et al. Seed amplification and neurodegeneration marker trajectories in individuals at risk of prion disease. *Brain*. 2023;146(6):2570-2583. doi:10.1093/brain/awad101
33. Makarava N, Chang JC, Molesworth K, Baskakov IV. Region-specific glial homeostatic signature in prion diseases is replaced by a uniform neuroinflammation signature, common for brain regions and prion strains with different cell tropism. *Neurobiol Dis*. 2020;137:104783. doi:10.1016/j.nbd.2020.104783
34. Chen Z, Kong Y, Zhang J, et al. Toward an early clinical diagnosis of MM2-type sporadic Creutzfeldt-Jakob disease. *Ann Clin Transl Neurol*. 2023;10(7):1209-1218. doi:10.1002/acn3.51802
35. Nagoshi K, Sadakane A, Nakamura Y, Yamada M, Mizusawa H. Duration of prion disease is longer in Japan than in other countries. *J Epidemiol*. 2011;21(4):255-262. doi:10.2188/jea.je20100085
36. Rus T, Mlakar J, Jamšek J, Trošt M. Metabolic brain changes can predict the underlying pathology in neurodegenerative brain disorders: a case report of sporadic Creutzfeldt-Jakob disease with concomitant Parkinson's disease. *Int J Mol Sci*. 2023;24(17):13081. doi:10.3390/ijms241713081
37. Mente KP, O'Donnell JK, Jones SE, et al. Fluorodeoxyglucose positron emission tomography (FDG-PET) correlation of histopathology and MRI in prion disease. *Alzheimer Dis Assoc Disord*. 2017;31:1-7. doi:10.1097/WAD.0000000000000188
38. Matías-Guiu JA, Guerrero-Márquez C, Cabrera-Martín MN, et al. Amyloid- and FDG-PET in sporadic Creutzfeldt-Jakob disease: correlation with pathological prion protein in neuropathology. *Prion*. 2017;11(3):205-213. doi:10.1080/19336896.2017.1314427
39. Liu S, Sun X, Ren Q, et al. Glymphatic dysfunction in patients with early-stage amyotrophic lateral sclerosis. *Brain*. 2024;147(1):100-108. doi:10.1093/brain/awad274
40. Dredla BK, Del Brutto OH, Castillo PR. Sleep and perivascular spaces. *Curr Neurol Neurosci Rep*. 2023;23(10):607-615. doi:10.1007/s11910-023-01293-z
41. Ringstad G. Glymphatic imaging: a critical look at the DTI-ALPS index. *Neuroradiology*. 2024;66(2):157-160. doi:10.1007/s00234-023-03270-2
42. Ding XB, Wang XX, Xia DH, et al. Impaired meningeal lymphatic drainage in patients with idiopathic Parkinson's disease. *Nat Med*. 2021;27(3):411-418. doi:10.1038/s41591-020-01198-1
43. Ringstad G, Eide PK. Cerebrospinal fluid tracer efflux to parasagittal dura in humans. *Nat Commun*. 2020;11(1):354. doi:10.1038/s41467-019-14195-x